Diamond & Related Materials 142 (2024) 110802

Contents lists available at ScienceDirect

Diamond & Related Materials

journal homepage: www.elsevier.com/locate/diamond

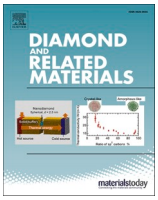

Erosion mechanisms of DLC coatings deposited on polyimide and silica substrates when exposed to a pulsed gas discharge

I. Zur [a,b,*], Y. Shmanay [a], J. Fedotova [a], G. Remnev [c], S. Movchan [d], V. Uglov [b]

[a] Institute for Nuclear Problems of Belarusian State University, st. Bobruiskaya 11, Minsk 220006, Belarus
[b] Belarusian State University, st. Bobruiskaya 5, Minsk, Belarus
[c] Tomsk Polytechnic University, st. Usov 4a, Tomsk, Russian Federation
[d] Joint Institute for Nuclear Research, st. Joliot-Curie 6, Dubna, Russian Federation

ARTICLE INFO

Keywords:
Diamond-like carbon
Resistive coating
Spark discharge
Surface erosion

ABSTRACT

The influence of spark discharges on the surface morphology and chemical composition of resistive diamond-like carbon (DLC) coatings designed to prevent breakdowns in gas electron multipliers (GEMs) has been studied. DLC coatings with thicknesses of approximately 200 nm and 66 nm were deposited in an inert argon atmosphere on polyimide substrates by high current pulsed magnetron sputtering and on silica (silicon oxide) substrates by vacuum arc method. Based on the analysis of images of optical and scanning electron microscopy, it was established that, the region of interaction between the gas discharge channel and the coating surface presents an accumulation of erosion craters with a characteristic linear size in the range of 20–40 μm. The value of current density passing in the region of interaction between the plasma in spark discharges and the sample is estimated to be of the order of 10^5 A/cm^2, which is sufficient to ablate the coating and create thermal stresses of magnitude ~4 GPa at the interface between the coating and the substrate. Thus, pulsed surface erosion, insufficient adhesive strength of the coating to the substrate, and poor thermal conductivity should be considered as the key reasons for destruction of the DLC coating.

1. Introduction

Progress in modern elementary particle physics largely depends on the functional characteristics of the detectors used [1,2]. To obtain correct data on the detected particles, it is necessary to ensure the stable functioning of the detectors throughout the entire period of operation. Breakdowns in gas electron multipliers (GEMs) of various types [3] are a serious problem due to the graphitization of the holes of the multiplying element, which leads to the failure of the detector.

To limit the discharge current, resistive coatings [4] can be used, which, on the one hand, will prevent breakdown and, on the other hand, will remove excess charge from the electron avalanche and thereby reduce the electron concentration in the gas to values below the critical ones. Diamond-like carbon (DLC) coating can be chosen as such a resistive material. DLC is characterized by a variable-range hopping conduction mechanism at room temperature [5,6], and a high surface electrical resistance (2–3 • 10^8 Ω/□). DLC coatings are usually a metastable form of carbon with a varying ratio of sp^2 to sp^3-hybridized bonds between carbon atoms [7].

Currently, several investigations are known to assess the possible application of various resistive coatings for solid-state detectors of charged particles [4]. There is also a study of thick GEM detectors (THGEM) [8], which shows that the highest gain is achieved in a detector with a resistive layer on the anode (~10^{11} Ω/□).

Protective coatings in detectors can be subject to destruction during long-term operation. So far, presently, much attention is paid to the study of the erosion of multilayer coatings such as CrN, CrAlN, and CrAlN/CrN [9] and thick coatings of DLC [10,11] by the impact of micro- and nanosized particles. Also, modification of the surface morphology of polyethylene terephthalate and polyurethane polymer coatings by atmospheric pressure discharges was considered in [12]. It was proven, in particular, that the treatment of a PET surface with a dielectric barrier discharge plasma leads to an increase in roughness and, as a consequence, adhesive properties [12].

At the same time, the effect of spark discharges on the surface morphology and chemical composition of the resistive DLC coating, as well as the erosion mechanisms, have not been studied. In this regard, the aim of this study is to identify the main mechanisms of degradation

* Corresponding author at: Institute for Nuclear Problems of Belarusian State University, st. Bobruiskaya 11, Minsk 220006, Belarus
E-mail address: zur.ilya01@gmail.com (I. Zur).

https://doi.org/10.1016/j.diamond.2024.110802
Received 27 February 2023; Received in revised form 3 December 2023; Accepted 6 January 2024
Available online 11 January 2024

under the influence of a spark discharge of DLC coatings deposited on polyimide (Pi) and silica (Si/SiO_2) substrates.

2. Experimental

DLC coatings with a thickness of ≈200 nm were deposited on Pi substrates by the method of high-current pulsed magnetron sputtering in an inert argon atmosphere without substrate heating at an operating pressure of $2.7 \cdot 10^{-3}$ Torr. The thickness of DLC coatings was controlled during evaporation with a quartz thickness monitor built into the magnetron chamber. Samples of DLC coatings on Si/SiO_2 substrates were deposited on the PVM-D installation by vacuum arc method with a pulsed electric arc evaporator at a pulse repetition frequency of 3 Hz, and operating pressure in the chamber of $\approx 10^{-3}$ Pa. The thickness of the samples was controlled by the number of voltage pulses, 1500, corresponding to a thickness of ≈66 nm. The measurement of the surface electrical resistance of the samples by the two-probe method showed that its values are in the range of 2 to $20 \bullet 10^6$ Ω/□.

Fig. 1 shows an experimental setup scheme for studying the effect of electrical discharges on the morphology of DLC coatings. It includes two electrodes (4 and 5) and a source of pulsed electrical voltage 6 with a shock capacitance $C = 2$ A•h (0.07 F), which makes it possible to achieve a current in the plasma channel of the spark discharge of the order of 10 A. A tungsten needle was used as the cathode, and an indium contact on the Pi or Si/SiO_2 substrate was used as the anode. The experiments were carried out in a sealed chamber with continuous circulation of the $Ar_{90}(CO_2)_{10}$ gas mixture, which corresponds to the working gas in the standard GEM detector.

Temperature of the samples were measured by thermal scanner Bosh GTC 400 C PROFESSIONAL. Integrated optical photographs of the afterglow of plasma channels were obtained using a welding screen (12 DIN dimming) and a wide-angle camera with a resolution of 108 Mp, an aperture of f/1.8, frame rate of 960 fps.

The electron and ion temperatures of the barrier discharge plasma were estimated by the Ornstein method. This method uses the relative intensities of spectral lines to calculate the temperature [13]. Plasma emission spectra were obtained with a fiber-optic two-channel spectrometer S150-2-3648 with a matrix of 1024 sensitive elements in two wave ranges 200–500 and 500–1000 nm with a spectral resolution of 0.25 nm. The resulting spectra were recorded without time resolution since the duration of the plasma afterglow is two times shorter than the minimum spectrum acquisition time.

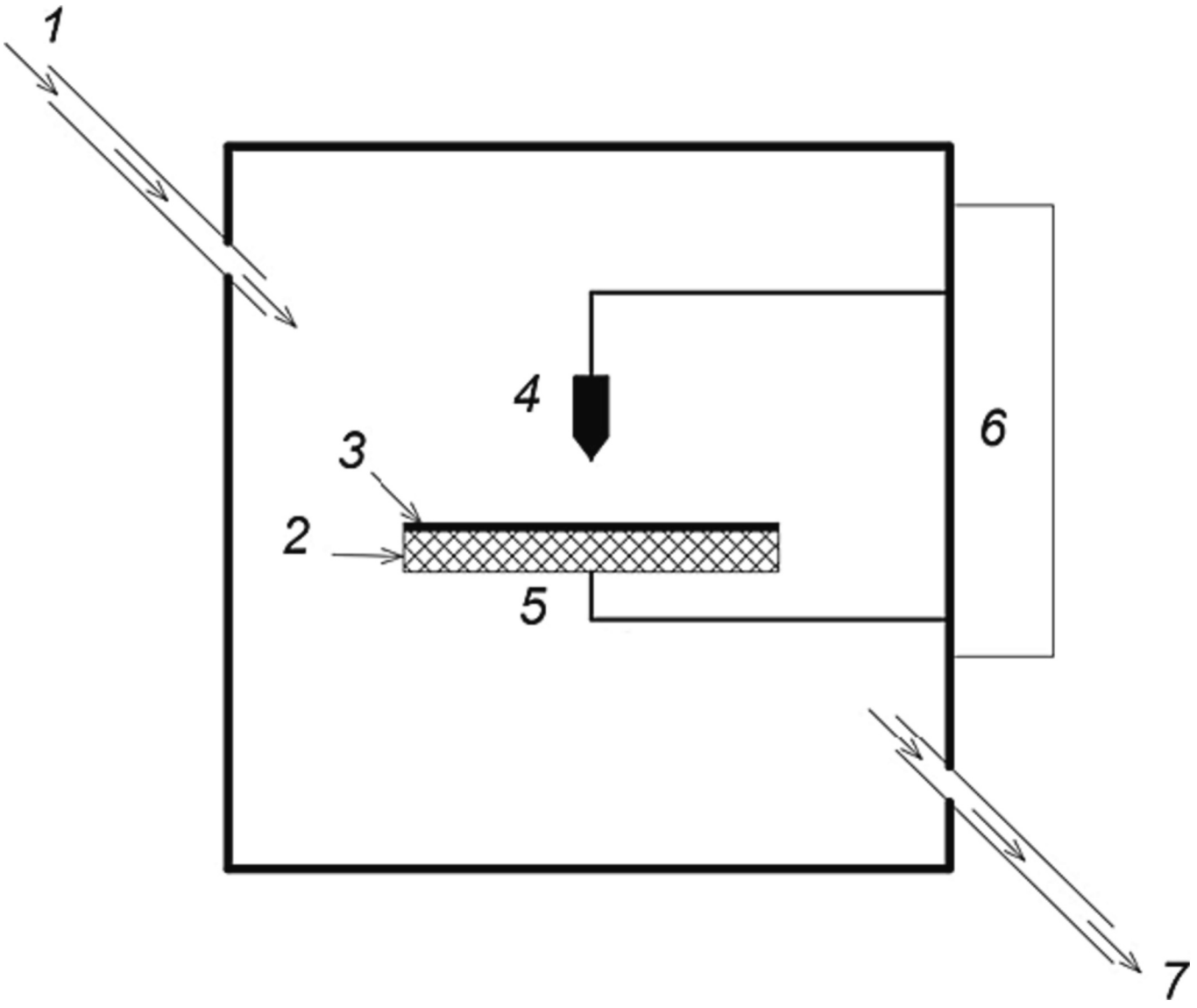

Fig. 1. Experimental setup scheme for studying the effect of a pulsed gas barrier discharge on a DLC coating.
1 and 7 – input and output of gas mixture, 2 – Pi or Si/SiO_2, 3 – DLC coating, 4 – cathode, 5 – anode, 6 – pulse voltage source.

The current amplitude values during the discharge were recorded using an oscilloscope Agilent Keysight 3034 and a low-inductance current shunt composed of metal oxide resistors MO-200 with a nominal electric resistance of 10^1 Ω and a power of 2 W.

The surface morphology of the samples after exposure to the discharge was studied by a scanning electron microscope (SEM) LEO-1455 VP at an accelerating field of 20 kV equipped with the energy-dispersive analyzer Aztec Energy Advanced X–Max 80, allowing for the estimation of chemical composition in the regions of erosion craters.

3. Experimental results and discussion

3.1. Effect of the spark discharge on the morphology and chemical composition of DLC coatings

The obtained integral photographs of the barrier discharge channel afterglows with a duration of the order $3 \bullet 10^{-3}$ s are presented in Fig. 2.

For DLC samples on a Pi substrate, a sliding discharge is observed (Figs. 2a, b), while for samples on a Si/SiO_2 substrate – a perforating discharge is found (Figs. 2c, d). In order to eliminate the influence of the geometrical parameters of the samples on the results obtained, square-shaped samples with rib lengths of 20, 30, and 40 mm were used. The observed shape and trajectory of the spark discharge plasma channel in the afterglow mode were the same for all samples.

An analysis of the typical emission spectrum in the entire available wavelength range, presented in Fig. 3, showed that the main contribution to the radiation is made by the excited neutral argon atoms Ar I and its singly charged Ar II ion; no spectral lines typical for ions of a higher ionization order were identified. The ion temperature, estimated by the method of relative intensities of spectral lines, is in the range of 0.14–0.24 eV. The minimum electron temperature equals 1.5 eV and was estimated as 10 % of the energy level of a neutrally excited atom [14] obtained from the spectrum. The maximum temperature was 2.7 eV and was estimated as 10 % of the energy required to produce a doubly charged argon ion, Ar III (27.68 eV).

The propagation of the plasma filaments along the spark channel during the sliding discharge led to the erosion of the DLC coating on the Pi substrate. In Fig. 4a, oblong-shaped damages can be observed, which are projections of plasma channels. Fig. 4b shows the SEM image in the secondary electron mode. A comparison of the photographs of the trajectories of the plasma channels in Fig. 2a with the observed damage of the coatings in Figs. 4a and b indicates their similarity.

For a DLC coating with a thickness of 66 nm on a Si/SiO_2 substrate, damage of the surface differs greatly from that for a Pi substrate. In this case, a barrier form of discharge is observed, when the discharge proceeds only in a gaseous medium and the surface electrical strength of the sample is too high for the formation of a discharge channel along the surface (sliding discharge). The SEM image in Fig. 5b shows that the characteristic linear size of the erosion crater is in the range of 20–40 μm. Optical images and the distribution of chemical elements (Fig. 6a) reveal that the DLC coating was fully removed in some localized areas after exposure to discharges.

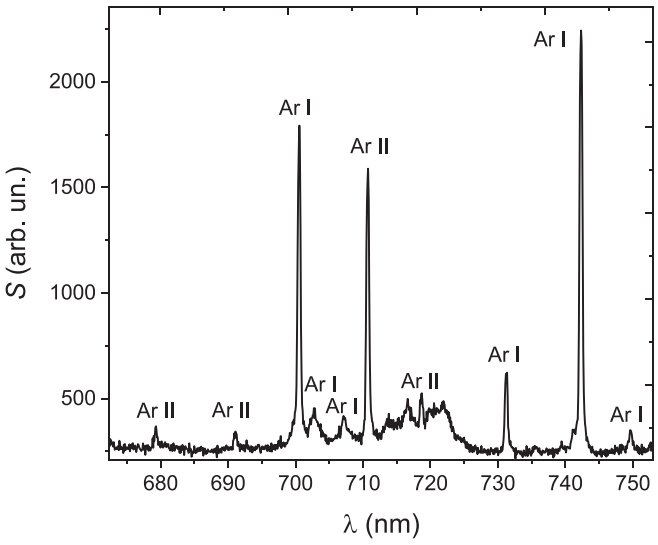

Fig. 3. The emission spectrum of the discharge plasma in the wavelength λ range of 675 … 755 nm, *S* – intensity without taking into account the spectral sensitivity, Ar I and Ar II - neutral atoms and singly charged argon ions.

The distributions of chemical elements in the area of erosion of the DLC coating on both substrates are shown in Fig. 6. Based on this analysis, it was found that the oxygen content decreases by an average of 5 % in the area of round-shaped erosion of the DLC coating on the Si/SiO_2 substrate (Fig. 6c) compared to other parts (Fig. 6a). This may indicate partial destruction of the native oxide on the DLC surface due to heating. The SEM image in Fig. 6b for the DLC sample on the Pi substrate shows characteristic elongated damage to the coating, resembling the discharge channel projection. Redistribution of elements in the vicinity of the discharge channel on the Pi substrate was not detected (Fig. 6d).

3.2. Estimation of contributions from possible erosion mechanisms of DLC coating

Let us analyze the possible erosion mechanisms of the DLC coating under the influence of a spark discharge. One of the mechanisms is pulsed erosion or ablation due to overheating of the region of interaction between the discharge channel and the coating. Fig. 5b shows

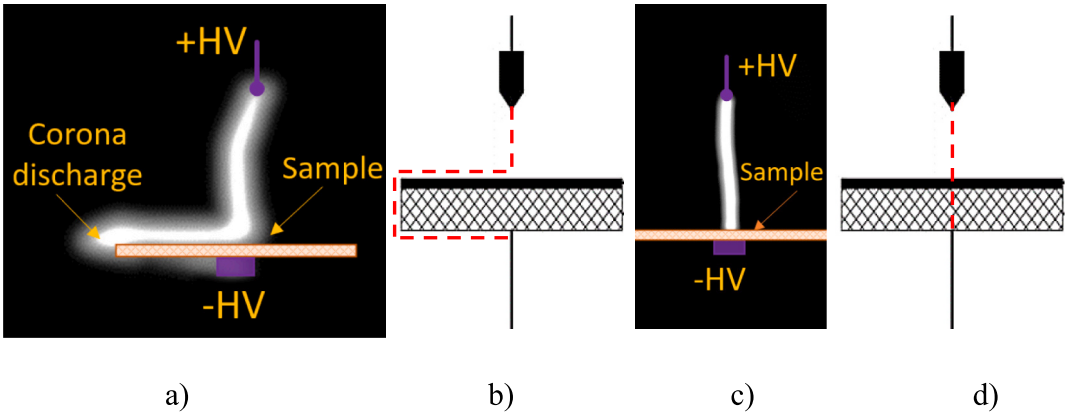

Fig. 2. Integrated optical photographs of afterglow (a and c) and a schematic representation (b and d) of plasma channels in experiments with samples on Pi (a and b) and Si/SiO_2 substrates (c and d)

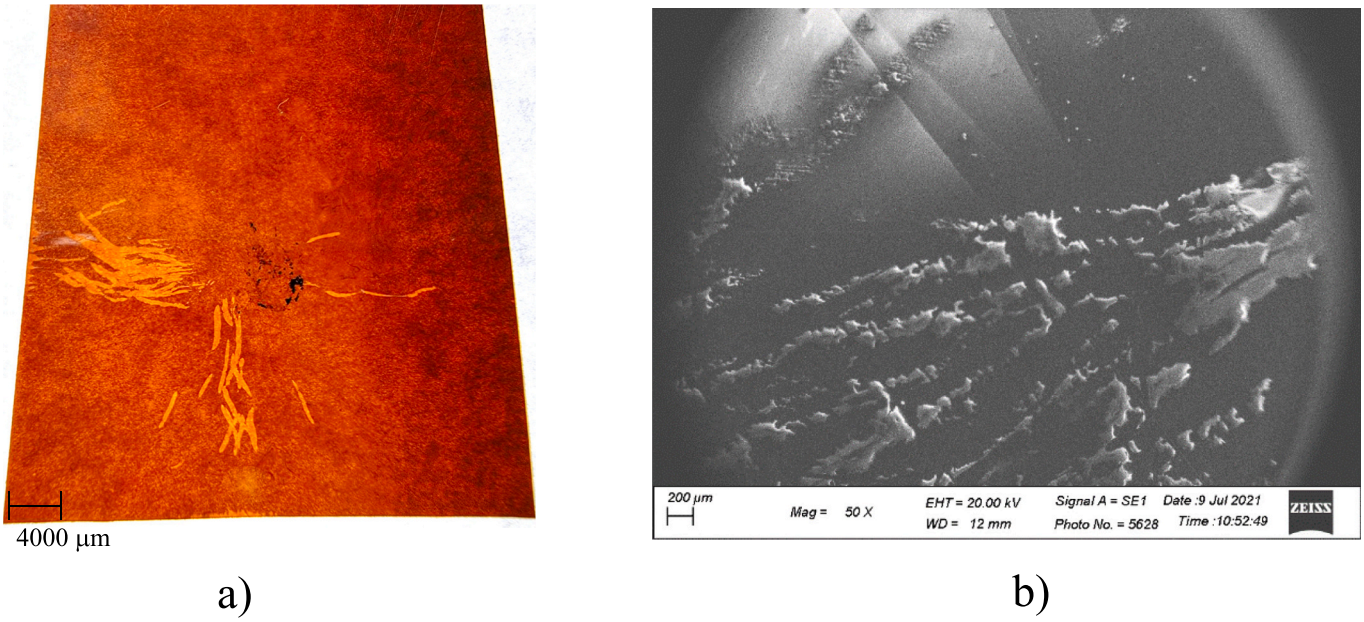

Fig. 4. Optical (a) and SEM (b) images of damages in the DLC coating on a Pi substrate after a sliding discharge.

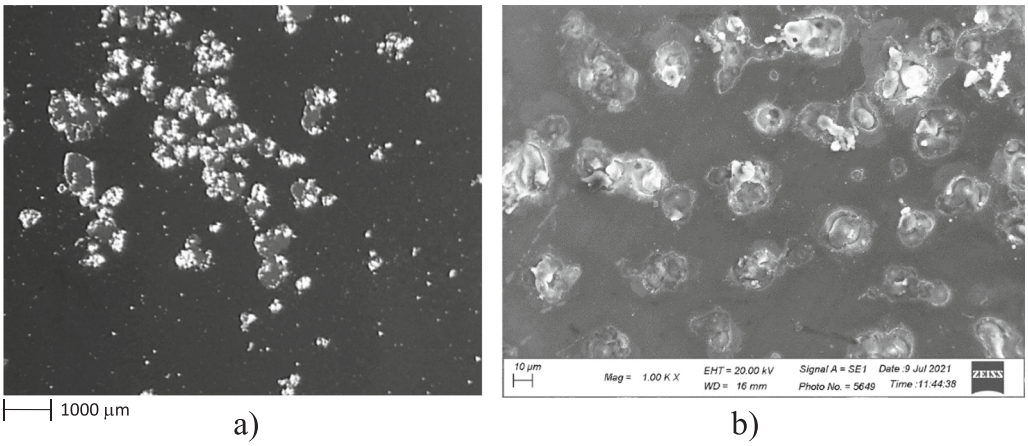

Fig. 5. Optical (a) and SEM (b) images of damages in the DLC coating on a Si/SiO_2 substrate after a perforating discharge.

agglomerations of round-shaped erosion craters with an average diameter of approximately 30 μm on the surface of the damaged DLC coating. The current density passing through the erosion crater area can reach a value of the order of 10^5 A/cm^2 (1 A per square of 30 × 30 μm^2), which significantly exceeds the energy of ablation of the coating material at its pulsed erosion.

Fig. 7 shows a temperature distribution T over the volume of the DLC coating along the scanning line in the area of breakdown measured by a thermal scanner for sliding and perforating discharges. It is seen that maximal values of T are 560 K and 385 K for the DLC on Pi (Fig. 7a) and on Si/SiO_2 (Fig. 7b) substrates, correspondingly. Note that the time constant of the thermal scanner is $8 \bullet 10^{-3}$ s, which is much longer than the discharge duration. Therefore, the T distributions in Fig. 7 are averaged over time so that local temperatures can be much higher and lead to local ablation of the DLC coating.

The second possible erosion mechanism for DLC coatings is its delamination from the substrate. It is caused by overheating during breakdown due to different thermal expansion coefficients (TECs) of the coating and substrate [15]–[18]. Besides, structural features of molecular chains in Pi [15], demonstrating their planar orientation, define the strong anisotropy of TEC. The values of TECs for the materials constituting the studied samples are summarized in Table 1.

Stresses in the film are mainly of residual mechanical and thermal origin that occur during local overheating. Thermal stresses in the film contain two components: shear stress σ_l (due to the difference in the TEC of DLC and substrate) and tensile stress σ_v (due to the difference in α_{sv} values for DLC and substrate). According to [16], they can be estimated from the system of Eq. (1):

$$\begin{cases} \sigma_l = \dfrac{E_f}{1-\nu_f}\left(\alpha_{s\,l} - \alpha_f\right)\left(T - T_{dep}\right) \\ \sigma_v = \dfrac{E_f}{1-\nu_f}\left(\alpha_{s\,v} - \alpha_f\right)\left(T - T_{dep}\right) \\ \sigma = \sqrt{\sigma_v{}^2 + \sigma_l{}^2} \end{cases} \quad (1)$$

where E_f and ν_f are Young's modulus and Poisson's coefficient of DLC, respectively; α_s and α_f are TEC of the substrate (s) and DLC coating (f), respectively; and T_{dep} is the temperature of the substrate during deposition (323 K).

Estimations show that for a DLC on a Pi substrate, the main contribution to the coating deformation comes from the vertical stress σ_v,

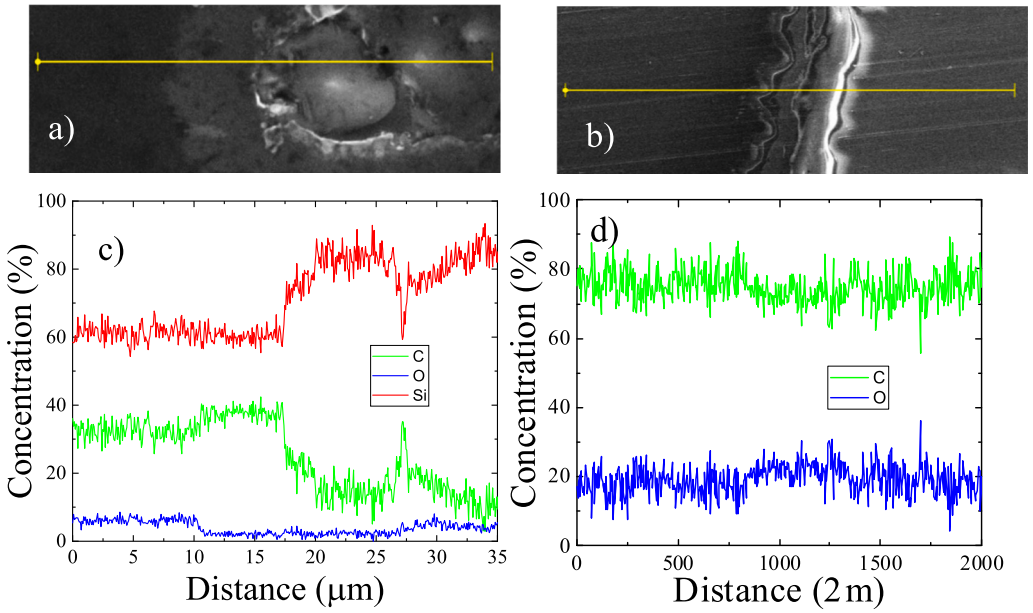

Fig. 6. SEM images (a, b) with distributions of chemical elements along the scanning line (c, d) in the erosion zone after exposure to the plasma channel on DLC coatings on Si/SiO_2 (a, c) and Pi (b, d) substrates

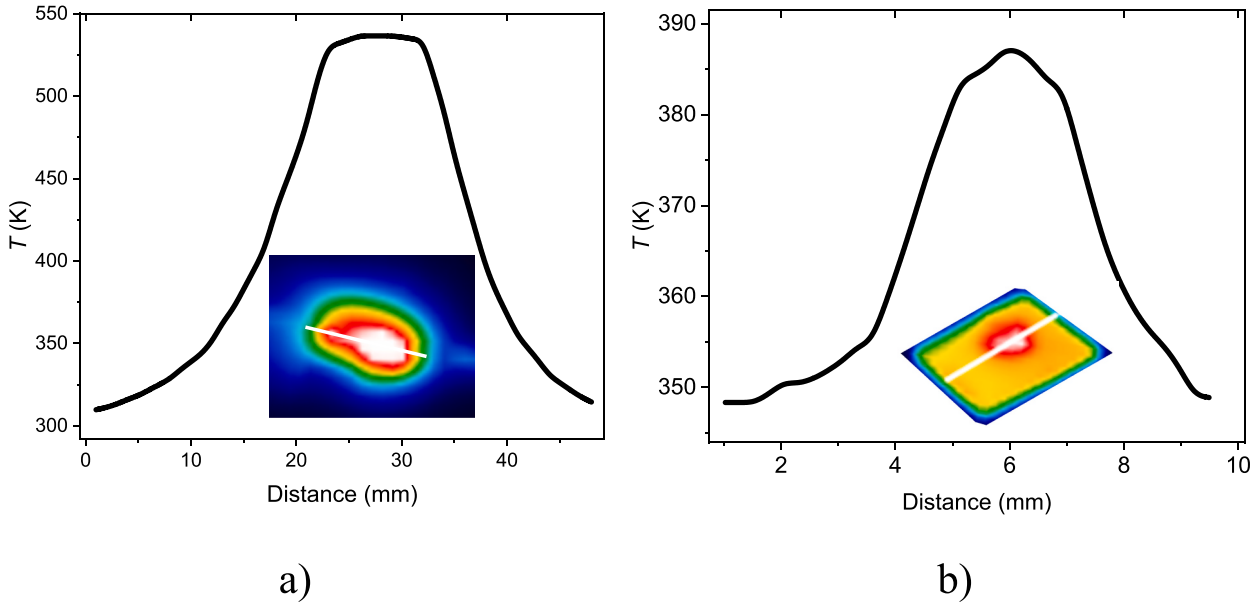

Fig. 7. The distribution of temperature *T* over the volume of the DLC coating along the scanning line, obtained using a thermal scanner with sliding (a) and a perforating discharge (b). The insets show 2D-distribution of *T*.

Table 1
Values of thermal expansion coefficients (TECs) for DLC coatings, polyimide (Pi), and Si/SiO_2 substrates. α_{sl} – lateral TEC, α_{sv} – vertical TEC.

Material	DLC	Pi, α_{sl}	Pi, α_{sv}	Si	SiO_2
TEC, 10^{-6} K^{-1}	3 [16]	9 [15]	110 [15]	3 [17]	0.5 [18]

which equals 4,1 GPa. Lateral stress σ_l comprises 0,24 GPa, that is not such a high value assuming that the difference between lateral TEC for the substrate and DLC coating differs by about 3 times. The resulting stress value has a positive sign, therefore, it is the expansion stress. For the DLC coating on the Si/SiO_2 substrate, compressive stresses are observed with a value of −0.1 GPa. However, the study [19] showed that the average normal stress and shear stress leading to flacking of the DLC coating were 7.76 KPa and 0.948 KPa, respectively. This is much less than the estimated thermal stresses, confirming definitely that their values are apparently sufficient for the delamination of the DLC coating from the substrate.

The evaluations also show that the sputtering by plasma filaments along the spark channel cannot be the origin of DLC coating erosion due to the small value of the ion energy (of the order of 0.25 eV as estimated from plasma spectral diagnostics) relative to the sputtering activation energy. In addition, the ion velocity is insufficient to reach the DLC surface during the discharge.

Thus, for both substrates, the destruction of the DLC coating is caused by both pulsed surface erosions under the action of a spark discharge and insufficient adhesion of the coating, which leads to a

delamination of the coating from the substrate.

4. Conclusion

The influence of a pulsed gas discharge on DLC coatings of 200 nm on Pi substrate and 66 nm thicknesses on Si/SiO_2 substrate is studied. To perform the experiments, a setup is developed that contains a pulsed electrical voltage generator, electrodes, and a sealed chamber for the $Ar_{90}(CO_2)_{10}$ inert medium. Two types of spark discharges are observed leading to DLC erosion, namely, sliding and perforating discharges for DLC on Pi and Si/SiO_2 substrates, correspondingly.

A detailed analysis of the morphology of the samples after exposure to spark breakdowns by optical microscopy and SEM reveals a violation of the morphology and chemical composition of the DLC surface. Complete destruction of the coating area is more likely to be observed during perforating discharges of DLC on Si/SiO_2 substrate with the characteristic damage linear size in the range of 20–40 μm.

In the case of sliding discharge, the structural integrity of the DLC coating on the Pi substrate is partially preserved, and the observed damages are space-localized and are projections of the plasma channels.

It has been established that the main contribution to the erosion of the DLC coating is associated with two mechanisms: flaking from the substrate due to the low adhesion strength of the coating to the substrate and ablation from the region of interaction of the plasma filaments in the discharge channel with the DLC coating. To increase the erosion resistance of DLC coatings to the effect of a gas discharge, it is necessary to reduce the difference between the TEC of the coating and the substrate, improve the coating's adhesive strength, increase their thermal conductivity due to the phonon contribution, and improve the density of sp^3 hybridized atoms in the coating [20].

CRediT authorship contribution statement

I. Zur: Conceptualization, Formal analysis, Writing – original draft, Writing – review & editing. **Y. Shmanay:** Formal analysis. **J. Fedotova:** Supervision, Writing – review & editing. **G. Remnev:** Investigation. **S. Movchan:** Funding acquisition, Validation. **V. Uglov:** Validation.

Declaration of competing interest

The authors declare that they have no known competing financial interests or personal relationships that could have appeared to influence the work reported in this paper.

Data availability

Data will be made available on request.

Acknowledgements

Authors acknowledge the financial support of Joint Institute for Nuclear Research (JINR) under contracts N08626319/201142470-74 (2021) and N08626319/2011293539-74 (2022).

The assistance in conducting experiments and fruitful discussions with Prof. A.K. Fedotov (INP BSU), Dr. A. Kharchanka (INP BSU), Dr. A. S. Fedotov (BSU) and Dr. D.A. Kotov (BSUIR) are gratefully acknowledged.

References

[1] D. Pierroutsakou, Gas detectors for nuclear physics experiments, EPJ Web Conf. 184 (Jan. 2018) 01015, https://doi.org/10.1051/epjconf/201818401015.
[2] M. Musacci, et al., Radiation tolerance characterization of Geiger-mode CMOS avalanche diodes for a dual-layer particle detector, Nucl. Instrum. Methods Phys. Res. Sect. Accel. Spectrometers Detect. Assoc. Equip. 936 (Aug. 2019) 695–696, https://doi.org/10.1016/j.nima.2018.10.078.
[3] A. Breskin, et al., Ion-induced effects in GEM and GEM/MHSP gaseous photomultipliers for the UV and the visible spectral range, Nucl. Instrum. Methods Phys. Res. Sect. Accel. Spectrometers Detect. Assoc. Equip. 553 (1–2) (Nov. 2005) 46–52, https://doi.org/10.1016/j.nima.2005.08.005.
[4] J. Metcalfe *et al.*, "Potential of Thin Films for use in Charged Particle Tracking Detectors," *ArXiv14111794 Hep-Ex Physicsphysics*, Nov. 2014, Accessed: Jan. 12, 2022. [Online]. Available: http://arxiv.org/abs/1411.1794.
[5] B. I. Shklovskii and A. L. Efros, "Dependence of hopping conduction on the impurity concentration and strain in the crystal," in *Electronic Properties of Doped Semiconductors*, B. I. Shklovskii and A. L. Efros, Eds., in Springer Series in Solid-State Sciences., Berlin, Heidelberg: Springer, 1984, pp. 137–154. doi:https://doi.org/10.1007/978-3-662-02403-4_6.
[6] Y. E. Shmanay, "Influence of diamond-like structure of nanosized layers on their electrical conductivity," presented at the 58th scientific conference of postgraduates, undergraduates and students of BSUIR, 2022, pp. 921–924. Accessed: Aug. 20, 2022. [Online]. Available: https://libeldoc.bsuir.by/handle/123456789/47667.
[7] J. Robertson, "Diamond-like amorphous carbon," Mater. Sci. Eng. R. Rep., vol. 37, no. 4–6, pp. 129–281, May 2002, doi:https://doi.org/10.1016/S0927-796X(02)00005-0.
[8] I. Vankov *et al.*, "Thick GEM with a resistive coating," Phys. Part. Nucl. Lett., vol. 10, no. 7, pp. 783–787, Dec. 2013, doi:https://doi.org/10.1134/S1547477114010191.
[9] H. Guo *et al.*, "Erosion behavior of CrN, CrAlN and CrAlN/CrN multilayer coatings deposited on Ti6Al4V," Surf. Coat. Technol., vol. 437, p. 128284, Feb. 2022, doi:https://doi.org/10.1016/j.surfcoat.2022.128284.
[10] V. Bonu, G. Srinivas, V. Praveen Kumar, A. Joseph, C. Narayana, and H. C. Barshilia, "Temperature dependent erosion and Raman analyses of arc-deposited H free thick DLC coating on Cr/CrN coated plasma nitrided steel," Surf. Coat. Technol., vol. 436, p. 128308, Apr. 2022, doi:https://doi.org/10.1016/j.surfcoat.2022.128308.
[11] S. J. McMaster, T. W. Liskiewicz, A. Neville, and B. D. Beake, "Probing fatigue resistance in multi-layer DLC coatings by micro- and nano-impact: correlation to erosion tests," Surf. Coat. Technol., vol. 402, p. 126319, Nov. 2020, doi:https://doi.org/10.1016/j.surfcoat.2020.126319.
[12] K. G. Kostov *et al.*, "Treatment of PET and PU polymers by atmospheric pressure plasma generated in dielectric barrier discharge in air," Surf. Coat. Technol., vol. 204, no. 18, pp. 3064–3068, Jun. 2010, doi:https://doi.org/10.1016/j.surfcoat.2010.02.008.
[13] V. Gorbunkov, V. Kositsyn, Estimation of the arc discharge plasma temperature of an electrothermal micromotor, Omsk Sci. Bull. 2 (3) (2018) 44–50, https://doi.org/10.25206/2588-0373-20182-3-44-50.
[14] V. Ivanov, M. Konyzhev, Determination of the electron temperature in microplasma discharges excited on a titanium surface, Plasma Phys. Rep. no. 6 (2012) 7, https://doi.org/10.1134/S1063780X13070143.
[15] G. Elsner, J. Kempf, J. W. Bartha, and H. H. Wagner, "Anisotropy of thermal expansion of thin polyimide films," Thin Solid Films, vol. 185, no. 1, pp. 189–197, Feb. 1990, doi:https://doi.org/10.1016/0040-6090(90)90018-9.
[16] F. C. Marques, R. G. Lacerda, A. Champi, V. Stolojan, D. C. Cox, and S. R. P. Silva, "Thermal expansion coefficient of hydrogenated amorphous carbon," Appl. Phys. Lett., vol. 83, no. 15, pp. 3099–3101, Oct. 2003, doi:https://doi.org/10.1063/1.1619557.
[17] H. Watanabe, N. Yamada, and M. Okaji, "Linear thermal expansion coefficient of silicon from 293 to 1000 K," Int. J. Thermophys., vol. 25, no. 1, pp. 221–236, Jan. 2004, doi:https://doi.org/10.1023/B:IJOT.0000022336.83719.43.
[18] H. Tada *et al.*, "Thermal expansion coefficient of polycrystalline silicon and silicon dioxide thin films at high temperatures," J. Appl. Phys., vol. 87, no. 9, pp. 4189–4193, May 2000, doi:https://doi.org/10.1063/1.373050.
[19] J. Zhang, B. He, X. L. Wei, and Z. W. Yuan, "Analyses of adhesion strength for DLC coating-silicon structure," Appl. Mech. Mater., vol. 197, pp. 717–721, Sep. 2012, doi:https://doi.org/10.4028/www.scientific.net/AMM.197.717.
[20] C. Wei and J.-Y. Yen, "Effect of film thickness and interlayer on the adhesion strength of diamond like carbon films on different substrates," Diam. Relat. Mater., vol. 16, no. 4–7, pp. 1325–1330, Apr. 2007, doi:https://doi.org/10.1016/j.diamond.2007.02.003.